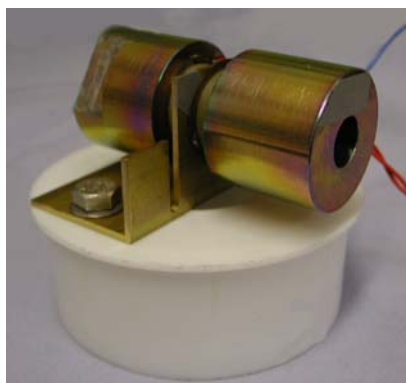


High Frequency Displacement and Dielectric Measurements in Piezoelectric Materials

There is a significant market for functional materials within the ultrasonics field, including applications such as ultrasonic cleaning, medical imaging and sonar. Here, the frequencies of operation are in the range kHz - MHz.

This Measurement Note provides an evaluation of high frequency measurement methods used to assess the performance of a simple sandwich Tonpilz-type sonar transducer. The aim being to correlate the measured high frequency displacement with another parameter which is simpler to measure in order to ascertain the requirements for optimum transducer performance. Particular emphasis is placed on detailing the experimental techniques used to achieve this.

The sandwich system was evaluated with three different piezomaterials under changing mechanical clamping conditions to determine the optimum transducer pre-stress level. High frequency displacement measurements were made at high field and were correlated to dielectric measurements made at low field - impedance - and high field - current. The pre-stress in the sandwich transducer was monitored using an instrumented bolt containing an optical fibre with Bragg grating. The resonant frequencies measured using each of the three methods were found to correlate closely. However, no relationship could be found between the displacement amplitude and the dielectric measurements with changing clamping load, which would enable the optimum pre-stress for a particular field level to be predicted. Recommendations are made for improvements to the sample and test protocol.



**M J Lodeiro, M G Cain
and M Stewart**

March 2002

INTRODUCTION

There are a wide variety of high frequency applications of piezoelectric functional materials operating in the range from 10 kHz to several MHz. These include:

- humidifiers,
- ultrasonic cleaning,
- ultrasonic welding,
- medical imaging/diagnosis and therapy,
- NDT e.g. C-scan,
- communications and optical devices e.g. SAWs, filters or relaxors,
- microactuators e.g. positioning systems,
- sonar.

As operating frequencies approach the ultrasonic regime, the measurements of strain or displacement required to determine improvements in application performance or optimise transducer design are increasingly difficult.

This is particularly the case at resonance – a state of ongoing oscillations which can be excited efficiently for a lower driving force – which is often poorly characterised due to the high frequencies and large amplitude displacements involved.

The aim of this work was to investigate measuring high frequency displacements at high field for an industrially relevant application (sonar) using a differential laser Doppler vibrometer, in order to optimise the transducer performance.

The basic assumption used was that the sound pressure waves produced underwater are directly proportional to the displacement of the transducer assembly, therefore the scenario for maximum transducer output corresponds with that for maximum displacement ¹.

These displacement data were then compared to low and high field dielectric measurements (impedance and current respectively), which are simpler to make and less expensive in equipment and operator time, in order to ascertain the validity of this technique as an effective alternative.

SANDWICH TRANSDUCERS

A simplified version of a real sonar transducer configuration was used to demonstrate the concept (Langevin/Tonpitz transducer, supplied by Sonardyne International Ltd).

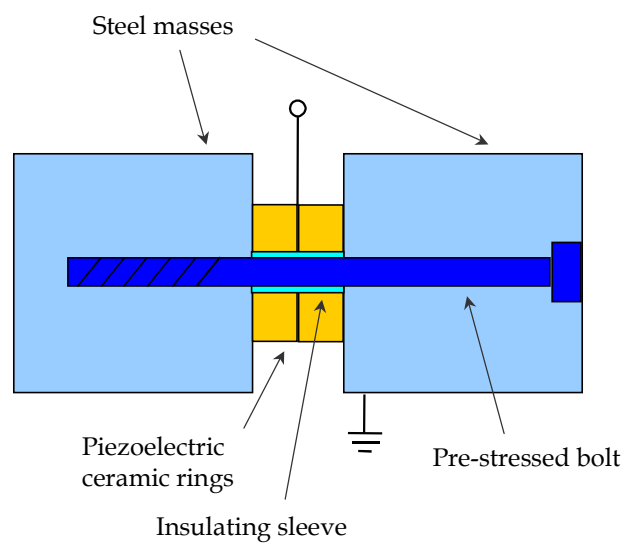


Figure 1 - Typical sonar sandwich transducer configuration.

The simplest form of pre-stressed transducer consists of a pair of piezoceramic rings poled in opposite directions, sandwiched between cylindrical metal end sections, as shown in Figure 1.

The assembly is placed under compression by means of a single central bolt (or several peripheral bolts). Thin copper electrode discs are located between the different components. The central electrode is live and both metal end masses are grounded. An insulating sleeve isolates the bolt, preventing it making contact with the live terminal.

How much compressive pre-stress should be applied to the system for optimum performance?

Currently, a mixture of experience, historical precedents and trial and error are employed to determine the tightening required. The charge is measured as the system is clamped, with a particular charge output being considered optimal. The designers need to know the driving voltage and clamping necessary to maximise output and minimise losses. These transducers are run at high voltage and pre-stressing leads to variations in transducer performance which may be due to shifts in the characteristic parameters of the piezoelectric material and/or changes in the coupling (effective contacting surface area) between different parts of the device.

In order to improve the basis for the choice of pre-stress level, the effect of a number of parameters were chosen to be

investigated/measured using the Tonpilz system:

- bolt torque/load,
- transducer displacement,
- impedance,
- resonant frequency,
- current,
- driving voltage,
- different materials.

In this example, the piezoelectric ceramic samples were nominally 20 mm external diameter, 8 mm internal diameter and 6 mm thick.

The piezomaterials chosen for study were PC4D, PC8 (both from Morgan Electro Ceramics Ltd, UK) and Channel 5400 (from Channel Products Inc, USA).

Measuring Bolt Pre-Stress

The obvious way to measure the bolt tightening level is using a torque wrench. However, this method is subject to inaccuracy due to the effect of friction between the surfaces being clamped together.

An alternative is to instrument the bolt using an optical fibre with a Bragg grating, as shown in Figure 2.

The grating is formed by periodic variations in the refractive index of the glass along the length of the fibre. The spatial period of these variations dictates the specific

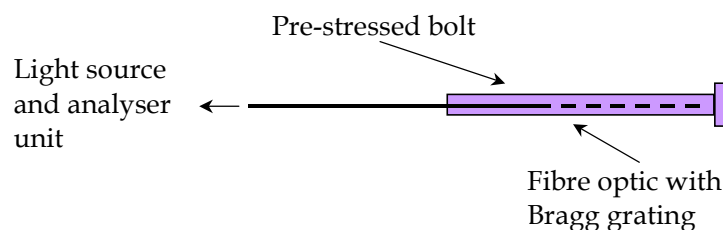


Figure 2 - Schematic of an instrumented bolt.

frequency of light which is selectively reflected when illuminated with white light.

Strain in the grating is thus sensed as a shift in the frequency of the light which is reflected, caused by the change in the spacing of the periodic refractive index variations which are altered by externally imposed strain.

An instrumented bolt was produced by drilling a 1.5 mm hole through the centre of the bolt along its entire length. An optical fibre with Bragg grating was then bonded within using a high strength, 2-part, room temperature cure epoxy adhesive.

The optical fibre was connected to an ElectroPhotonics Corporation FLS 3100 module for illumination and signal conversion² and the signal was subsequently displayed real-time on a PC via a NI DAQ card (AI-16XE-50, 200kS/s, 16 bit).

Once instrumented, it was necessary to correlate the output from the fibre optic strain sensor with the load on the bolt. This was achieved by loading the bolt in tension using a purpose-built rig with a calibrated Instron 1250 hydraulic test machine and load cell. The fibre signal was monitored and recorded in conjunction with the applied load, producing a trace such as that shown in Figure 3.

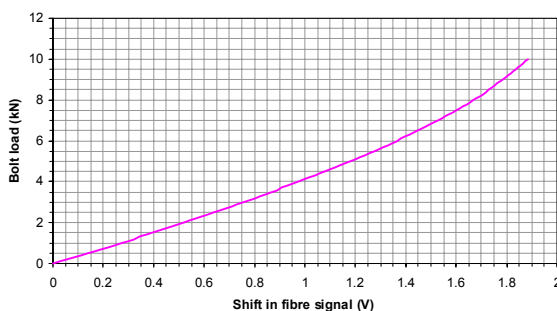


Figure 3 - Typical fibre output calibration trace.

This calibration was performed dynamically to 10 kN over five complete loading/unloading cycles to check for consistency.

Notes:

- The grating is highly temperature sensitive so a controlled environment or constantly monitored local temperature is required to ensure accurate strain measurements.

When compared with the load induced in the bolt for different torque levels, seen in Figure 4, it was noted that the direct tensile load on the bolt did not increase linearly with applied torque, as measured using the torque wrench. Thus as the clamping load increased, the torque increased disproportionately due to the increased frictional force between parts, without increasing the direct clamping load to the same extent. The two separate torque tests shown in Figure 4 also highlight the variability in the actual loads achieved for any particular torque level.

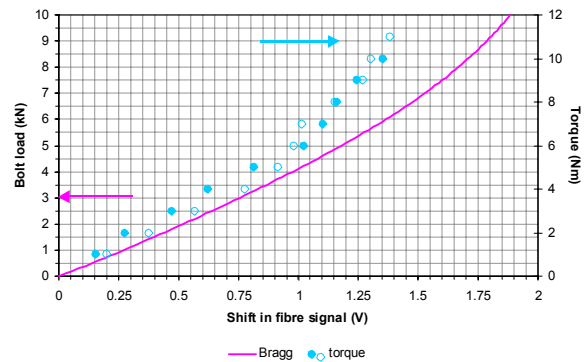


Figure 4 - Comparison between actual bolt load and torque level loading.

It was also noted that once tightened to a particular desired load level, the strain signal in the fibre decayed rapidly with time, as shown in Figure 5. Although some relaxation in the bolted assembly can be expected, the additional contribution was probably related to creep in the adhesive or the cladding surrounding the fibre and can be seen to be load dependent.

Thus the load in the bolt was determined from the initial change in fibre output signal, immediately following tightening, and subsequent changes in the fibre output with time were ignored.

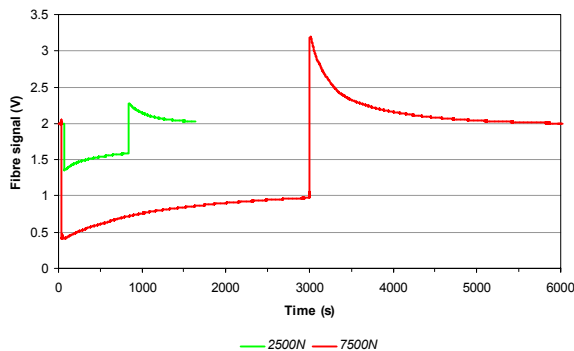


Figure 5 - Decay in fibre signal due to creep at different load levels.

Notes:

- The creep problem could be reduced by removing the fibre cladding prior to adhesion and/or drilling a thinner hole and therefore creating a thinner layer of adhesive around the fibre.

High Field Measurements

In summary, both displacement, and current data with drive frequency were collected and recorded to PC using LabView for different clamping loads (0.5 – 7.5 kN), different peak-peak driving voltages (50 – 200 V) and different materials.

Measuring Displacement

The displacement of the transducer was determined using a Doppler interferometer. The dual differential fibreoptic POLYTEC system (OFV 3001 controller and OFV 512 sensor head) is capable of measuring both displacement and velocity at high frequencies. The measurement set-up is

shown in Figure 6.

The sandwich transducer was mounted on a support, located at the nominal nodal position between the two piezoceramic rings. The surfaces of all of the component parts of the transducer were cleaned with isopropanol to remove grit and debris prior to assembly.

An HP 4192A LF impedance analyser (gain phase analyser/lock-in amplifier) was used as a frequency generator, sweeping up between 5 and 20 kHz at 50 Hz intervals. This signal was fed into a Brüel and Kjær type 2713 power amplifier which applied a sinusoidal AC voltage to the live electrode on the sample causing the end masses to vibrate symmetrically about the static node.

The reference beam of the laser vibrometer was sighted at the nodal position and the measuring beam was positioned on the front face of the metal end section, thus half the total displacement was measured.

It was necessary to ensure good alignment and focussing of the beams on the transducer and to electrically and mechanically isolate the system to minimise noise. To help achieve this, the signal from the vibrometer was monitored using a lock-in technique with the drive signal (having been reduced by a factor of ten using a voltage divider) being used as the reference frequency.

Notes:

- In order to change materials, the fibre had to be cut and re-spliced each time.
- A diffuse-reflecting self-adhesive tape was used as a laser target on the sample.

Measuring Current

The current generated by the transducer was measured using a Tektronix CT2 current transformer. The current probe set-up is also shown in Figure 6.

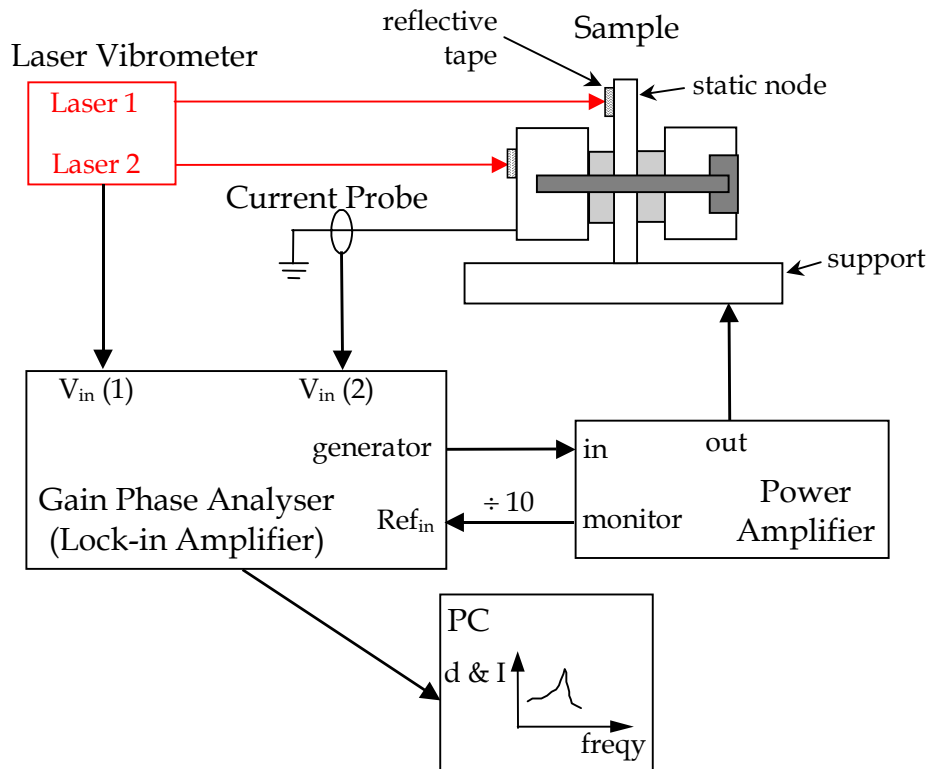


Figure 6 - Schematic of high field displacement and current measurement set-up.

Low Field Impedance Measurements

The impedance and phase angle of the transducer assembly was measured at 1 V peak-peak oscillation amplitude, between 5 and 20 kHz at 50 Hz intervals, using an Agilent 4294A Precision Impedance Analyser. The low field data was recorded with drive frequency to PC using LabView.

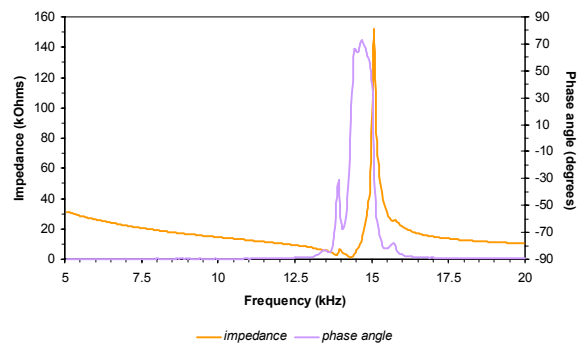


Figure 7 - Typical impedance and phase angle measurements at low field (example from PC4D at 4kN bolt load, 1 V pk-pk).

Results

High and Low Field Dielectric Results

An example of the low field dielectric raw data (impedance and phase angle) can be seen in Figure 7.

These raw data traces show an impedance minimum at the resonant frequency and a maximum at the anti-resonant frequency. Similarly the phase angle shows a peak bordered (points of inflection) at these two

characteristic frequencies.

The change in the resonant and anti-resonant frequencies with increasing clamping load level is shown in Figure 8. The repeatability of the data can be seen from the additional points.

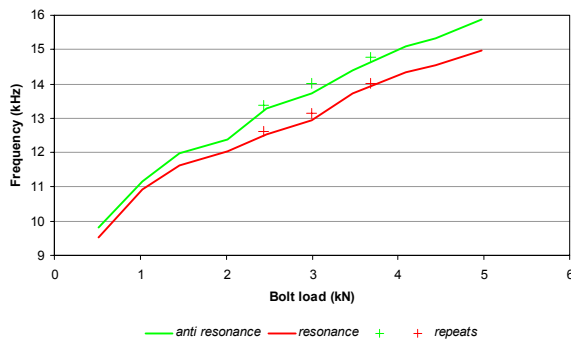


Figure 8 - Resonant and anti-resonant frequencies for PC4D.

As has been seen by other studies^{3,4}, the resonant and anti-resonant frequencies not only increase with increasing pre-stress but also diverge.

An example of the high field dielectric raw data (current) can be seen in Figure 9. This raw data trace shows a dramatic increase in the current generated within the transducer at resonance. This correlates to the expected increase in the displacement of the transducer at resonance.

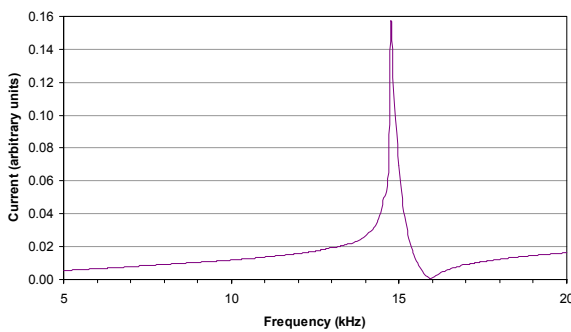


Figure 9 - Typical current measurement at high field (example from PC8 at 5kN bolt load, 200 V pk-pk).

The dependence of the current resonance with driving voltage amplitude can be seen in Figure 10. This shows a marked, if small, reduction in the resonant frequency with increasing drive voltage.

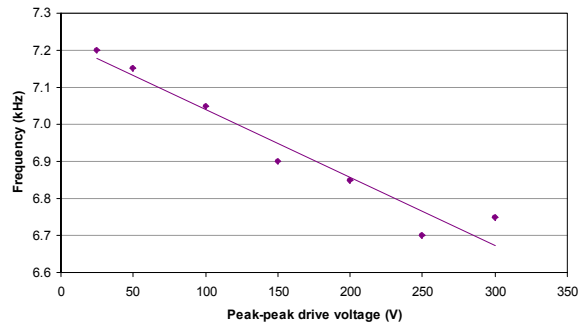


Figure 10 - Relationship between current resonance frequency and driving voltage amplitude (example from PC8 at <500N bolt load).

Comparisons of these two measurements of resonant frequency for different clamping load levels are shown for two materials in Figures 11 (a) and (b). These show a good correlation between the resonance data using the two techniques.

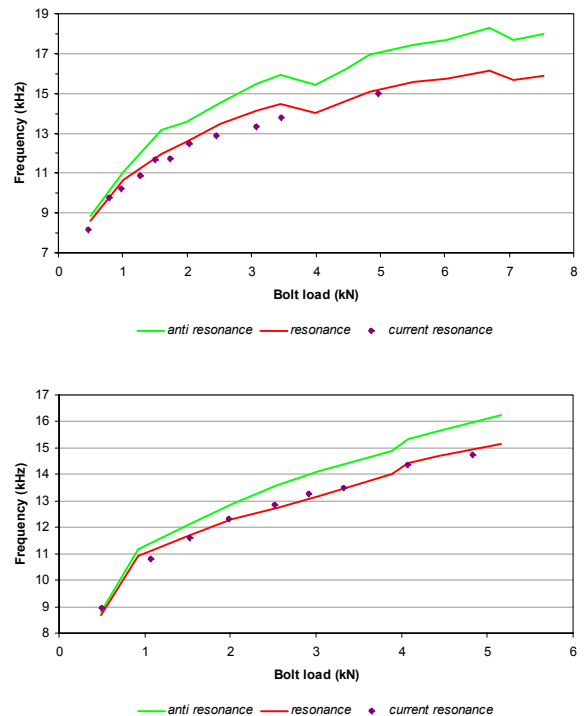


Figure 11 - Comparisons between resonance and anti-resonance impedance data and current resonance data with increasing clamping load: (a) Channel 5400 and (b) PC8.

Vibrometer Displacement Results

An example of the vibrometer displacement data at high field can be seen in Figure 12. These raw data traces show the complex nature of the displacement response of the transducer assembly and the maximum amplitude displacement evident at the resonant frequency.

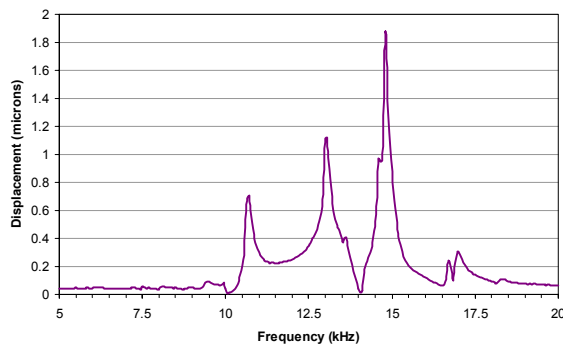


Figure 12 - Typical vibrometer displacement measurements at high field (example from PC8 at 5kN bolt load, 200 V pk-pk).

Comparison of this technique with the determination of resonance using current data are shown in Figure 13. These show a good correlation between all three techniques.

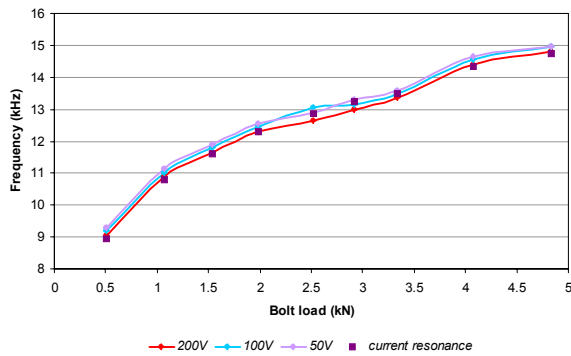


Figure 13 - Comparisons between resonance from current and displacement data with increasing clamping load for PC8.

A similar relationship to that shown for current resonance frequency and driving voltage (§ Figure 10) can be seen between the displacement resonance data and the driving voltage. Again there is a small reduction in resonant frequency with increasing drive voltage amplitude.

The maximum displacement at resonance with increasing pre-stress level is shown in Figure 14 (a) and (b). These show that in order to increase the maximum (resonance) transducer displacement output the applied field levels need to be increased. With respect to pre-stress, an optimum value is evident in each case.

These graphs also show a difference in the behaviour of the different materials: PC4D shows a reduction in the optimum clamping load with increasing drive voltage whilst PC8 has a constant optimum pre-stress level regardless of the amplitude of the drive voltage applied.

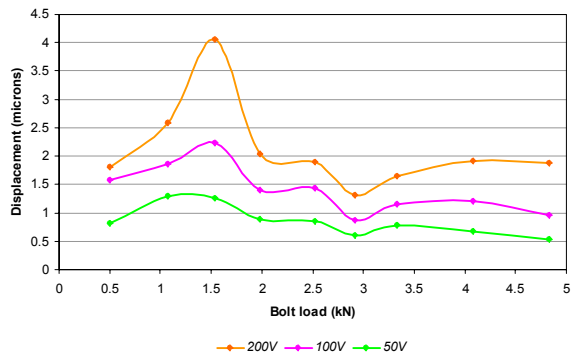
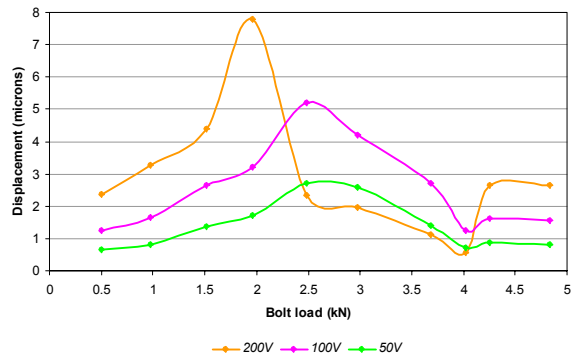


Figure 14 - Relationship between displacement and pre-stress (bolt clamping load) for different drive voltages: (a) PC4D and (b) PC8.

The displacement amplitude at the resonance frequency with increasing applied voltage does not increase linearly. This is again more marked for the PC4D than the PC8, as can be seen in Table 1

Table 1 – Effect of Field Level on Maximum Resonance Displacement at Optimum

Sample Material	Applied Drive Voltage		
	200 V	100 V	50 V
PC4D	7.8	5.2	2.8
PC8	4.1	2.3	1.4

However, the data for Channel 5400 showed unusual behaviour.

This was due to a number of factors:

- The transducer assembly was loosened between each load level measurement and re-tightened to the next load.
- The non-parallelism of the piezoceramic rings.

The contact area between the piezoceramic and the rest of the sandwich assembly is very important. Any imperfections on any of the surfaces will reduce the contact area, changing the local stress levels within the piezoelectric rings for nominally identical bolt pre-stresses and thus the measured displacement. This can be seen in Figures 15 and 16 (a) and (b).

Figure 15 shows the results of a surface topography investigation of the piezoceramic rings used in the investigation using laser profilometry. The non-parallel nature of the Channel 5400 rings is easily apparent.

Figures 16 (a) and (b) show the effect of this non-uniform cross-section on the vibrometer results. When the transducer assembly is tightened and repeat measurements are made, the displacement output is almost

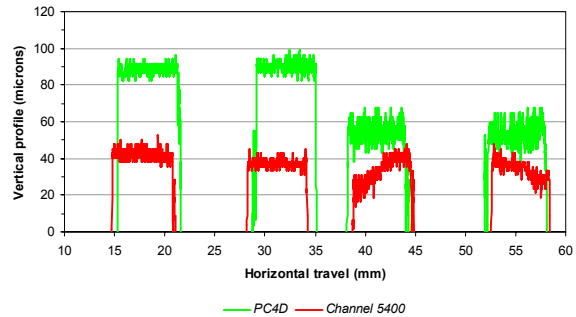


Figure 15 - Surface profiles of PC4D and Channel 5400 rings.

identical each time. When the transducer assembly is tightened and then loosened between experiments and the active piezoceramic rings are rotated as a result, the displacement output is much less consistent.

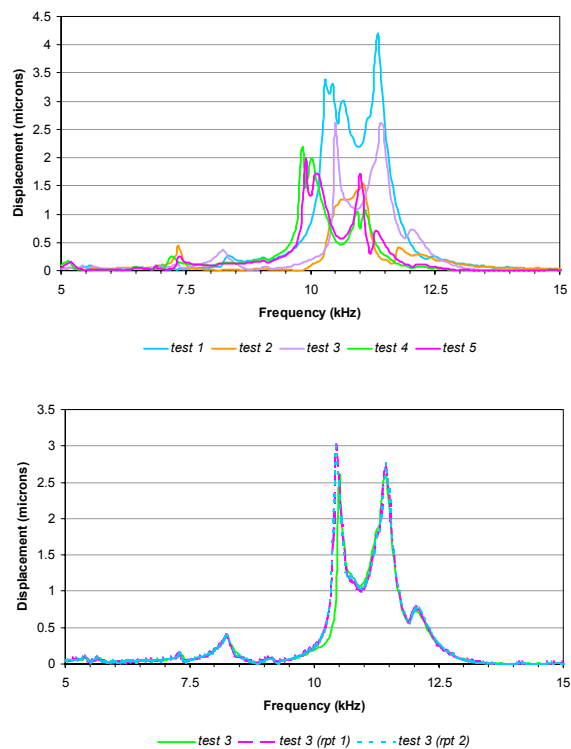


Figure 16 - Raw vibrometer displacement data for PC8 at 1.5 kN pre-load and 200V: (a) rotating piezo rings between each test and (b) repeats with no changes to set-up.

CONCLUDING REMARKS

There is a direct correlation between the resonance frequency determined from the low field impedance measurements and the high field displacement and current measurements. There seems to be, however, no simple correlation between the measurements of displacement amplitude at high field and those of low or high field dielectric properties in locating the optimum pre-stress level to give maximum displacement for a particular drive voltage.

Recommendations:

- Ensure parallelism and cleanliness of contacting surfaces.
- High applied fields are required to ensure displacement sweeps are less noisy and above the detection limit of the vibrometer.
- Improve creep performance of instrumented bolt.
- Place copper electrodes between every pair of contacting surfaces to accommodate imperfections and provide more uniform stressing.
- Improve sample support structure for better measurements.
- Improve system of location and alignment of sample for laser vibrometer measurements.

References

1. *M. G. Cain and M. Stewart, "Measurement of the surface displacement in 1-3 piezocomposites", NPL Report MATC (A) 94, April 2002.*
2. *M. Stewart and M. G. Cain, "Optical sensor characterisation and calibration device for integrated optical systems", NPL Report MATC (A) 57, September 2001.*
3. *F. J. Arnold and S. S. Mühlen, "The mechanical pre-stressing in ultrasonic piezotransducers", Ultrasonics 39, 2001, 7-11.*
4. *F. J. Arnold and S. S. Mühlen, "The resonance frequencies on mechanically pre-stressed ultrasonic piezotransducers", Ultrasonics 39, 2001, 1-5.*

Acknowledgements

The research reported in this Measurement Note was carried out by NPL, as part of the 'Characterisation and Performance of Materials Programme', funded by the Engineering Industries Directorate of the UK Department of Trade and Industry. The authors would like to acknowledge the contributions and assistance of Richard Shaw at NPL and Dick Hazelwood at Sonardyne International Ltd.

For further information contact:

Markys G. Cain
Sensors and Functional Materials
NPL Materials Centre
National Physical Laboratory
Queens Road
Teddington
Middlesex
TW11 0LW
Telephone: 020-8977 3222 (*switchboard*)
Direct Line: 020-8943 6599
Facsimile: 020-8943 2989

E-mail: markys.cain@npl.co.uk
Website: <http://www.npl.co.uk/npl/cmmt/functional/index.html>

© Crown Copyright 2002. Reproduced by permission of the Controller of HMSO.